



OPEN IFITMs exhibit antiviral activity against Chikungunya and Zika virus infection *via* the alteration of TLRs and RLRs signaling pathways

Nuttamonpat Gumpangseth^{1,2}, Paola Mariela Saba Villarroel^{1,2}, Abibatou Diack³, Thanaphon Songhong^{1,2}, Sakda Yainoy¹, Rodolphe Hamel^{1,2,3}, Wipaporn Khanom³, Phanit Koomhin^{4,5}, Chuchard Punsawad⁵, Anon Srikiatkachorn^{6,7}, Dorothée Missé³, Phoonthawee Saetear^{8,9} & Sineewanlaya Wicht^{1,2}✉

Chikungunya virus (

antiviral drugs or vaccines to combat this infection. Here, we demonstrate that interferon-induced transmembrane proteins (IFITMs), including IFITM1, IFITM2, and IFITM3, which are interferon-stimulated genes (ISGs), inhibit

Overexpression of IFITMs in cells restricts viral infection, whereas knockdown of IFITMs enhances viral infection. IFITMs overexpression causes a substantial upregulation of antiviral genes, namely TLR3, TLR7, TLR8, and TLR9, and their downstream signaling molecules such as TRADD, IRAK1, TRAF6, and MAP3K7, involved in TLRs signaling pathways. Furthermore, the DHX58 gene encoding the LGP2 protein, a negative regulator of RIG-I in RLRs signaling pathways, was downregulated in the overexpressed cells. Transcription factors including interferon regulatory factors (IRF) 3/5/7, which are downstream signaling components of both TLR and RLR signaling pathways, were also upregulated, resulting in enhanced IFNs signaling. IFITMs not only inhibits the early and late stages of viral infection but can also alter the antiviral innate-immune response to restrict

Additionally, IFITMs exhibit their antiviral activity against Zika virus (ZIKV). Altogether, these results show the broad-spectrum antiviral property of IFITMs against arboviruses in foreskin cells.

Keywords Chikungunya virus, Zika virus, IFITMs, Arbovirus, TLRs and RLRs signaling pathways

Chikungunya virus (CHIKV) is an arbovirus of the *Togaviridae* family, *Alphavirus* genus, transmitted mainly by *Aedes aegypti* and *Aedes albopictus*. It was first isolated in Tanzania in 1952, and currently, CHIKV cases have been reported in more than one hundred countries worldwide. Most patients suffer from polyarthralgia and myalgia that can persist for months or years, impacting their quality of life. Since no licensed drugs or vaccines are currently available, treatment of CHIKV infection focuses on supportive care, and prevention on mosquito vector control strategies and personal protection against mosquito bites^{1,2}. During a viral infection, the host innate immune response is triggered as an early defense mechanism to restrict viral infection. Pattern-recognition-receptors (PRRs) in the infected cells such as toll-like receptors (TLRs) and retinoic acid-inducible gene I (RIG-I) receptors, recognize viral components and trigger a downstream signaling cascade that further promotes expression and phosphorylation of several transcription factors involving Interferon regulatory factors (IRFs), nuclear factor kappa-light-chain-enhancer of activated B cells (NF-κB), and activator protein 1 (AP-1),

¹Department of Clinical Microbiology and Applied Technology, Faculty of Medical Technology, Mahidol University, Nakhon Pathom, Thailand. ²Viral Vector Joint unit and Joint Laboratory, Mahidol University, Nakhon Pathom, Thailand. ³MIVEGEC, Univ. Montpellier, CNRS, IRD, Montpellier, France. ⁴Center of Excellence in Innovation on Essential Oil, Walailak University, Nakhonsithammarat, Thailand. ⁵School of Medicine, Walailak University, Nakhonsithammarat, Thailand. ⁶Department of Cell and Molecular Biology, Institute for Immunology and Informatics, University of Rhode Island, Providence, Rhode Island, USA. ⁷Faculty of Medicine, King Mongkut's Institute of Technology Ladkrabang, Bangkok, Thailand. ⁸Flow Innovation-Research for Science and Technology Laboratories (Firstlabs), Bangkok, Thailand. ⁹Department of Chemistry, Center of Excellence for Innovation in Chemistry, Faculty of Science, Mahidol University, Rama 6 Road, Ratchatewi, Bangkok, Thailand. ✉email: sineewanlaya.wic@mahidol.ac.th

resulting in the production of interferons (IFNs) and other cytokines^{3,4}. Type I interferon signaling pathway is of the essential innate immune pathways that protects against viral infection through the expression of interferon-stimulated genes (ISGs) with antiviral activity⁵. Among ISGs, the immune-related interferon-induced transmembrane proteins (IFITMs), including IFITM1, IFITM2, and IFITM3, are transmembrane proteins that have been demonstrated to be upregulated following influenza A virus (IAV) infection in dendritic cells⁶, as well as infection of severe acute respiratory syndrome coronavirus 2 (SARS-CoV-2) in human patients^{7,8}, suggesting their role in the human immune response against viral infection^{9,10}. IFITM1 was first demonstrated to exert antiviral activity against vesicular stomatitis virus (VSV) in 1996¹¹; since then, a wide range of viruses have been reported to be inhibited by IFITM1, IFITM2, and/or IFITM3 proteins. However, the underlying mechanism of the antiviral activity of IFITMs is still unclear. They have been demonstrated to disrupt viral infection at the early stage through several means, including decreased membrane flexibility¹², induced lipid accumulation¹³ and being incorporated in the viral envelope, resulting in a reduction of virion infectivity¹⁴. IFITMs have been shown to exert different inhibitory effects in different cell types^{15,16}, suggesting a cooperation between IFITMs and other cell type-specific proteins during viral infection. Some reports studying IFITMs-deficient mice revealed the modulatory effect of IFITMs on cytokines that regulate cellular immunity, including NK cells and T helper 2 (Th2) cells^{17,18}. However, studies of the effect of IFITMs on the human innate immune response remain limited.

This work aims to study the effects of IFITM proteins on CHIKV infection and their impact on the human antiviral innate immune response during CHIKV infection. This study used human skin fibroblast as a model. Fibroblasts are located in the basal membrane layer, which is the site of virus inoculation and are permissive to CHIKV^{19,20}. As expected, IFITM1, IFITM2, and IFITM3 have antiviral effects against CHIKV infection in human skin fibroblasts. Furthermore, our study on the impact of IFITMs on the innate immune pathways in response to viral infection revealed a substantial upregulation of *TLRs* genes and a downregulation of *DHX58* gene in TLR and RLR signaling pathways, as well as enhanced expression of *IFNA1*, *IFNA2* and *STAT1* in the IFN pathway. Moreover, investigation of the effect of IFITMs on another arbovirus infection, Zika virus (ZIKV), demonstrated the broad-spectrum antiviral properties of IFITMs in human skin fibroblasts.

Results

HFF-1 cells were transfected with IFITM1, IFITM2 and IFITM3 plasmids at various concentrations. Cells transfected with plasmids at concentrations of 0.01 μg and 0.1 μg showed viability above 80%, whereas at a concentration of 1 μg , showed low cell viability compared to the control (Supplementary Fig. S1A). RT-qPCR and western blot analysis showed that all IFITM proteins were overexpressed in HFF-1 cells at both RNA and protein levels (Supplementary Fig. S1B and S1 C).

IFITMs exert antiviral properties against Chikungunya virus infection

To examine the effect of IFITMs on CHIKV infection, cells were transfected with IFITM plasmids and subsequently infected with CHIKV at MOI of 1. The inhibition of viral infection was analyzed by quantifying viral RNA and virus particles. Both viral RNA and virus particle production were completely abrogated (~100%) in all IFITMs overexpressing cells compared to plasmid control cells at 24- and 48-hour post-infection (hpi) (Fig. 1A and B). The data indicated that IFITM1, IFITM2, and IFITM3 equally constrain CHIKV infection in human skin cells.

IFITMs modulate Chikungunya virus infection

The effect of IFITMs on CHIKV infection was investigated in IFITM1, 2, or 3 knockdown cells. Endogenous IFITMs were silenced using a non-toxic concentration of 80 nM of specific siRNA (Fig. 2A). To confirm the expression level of IFITM1, 2, or 3 knockdown cells in both 24 and 48 h, RT-qPCR was used to quantify the RNA level compared to siControl knockdown cells (Supplementary fig. S3). Although the expression levels of all IFITMs were not different, RT-qPCR and plaque assay results showed that siIFITM-1 did not affect CHIKV replication, while siIFITM-2 and -3 transfected cells had a significant increase in CHIKV viral RNA and infectious viral particles compared to control cells (Fig. 2B and C).

The outcomes derived from both extrinsically overexpressed and knockdown cell models indicate that, despite IFITM1 exhibiting the highest expression level among all IFITMs, their antiviral properties against CHIKV are uniformly effective. Conversely, the silencing of IFITM1 in cells did not exert any observable impact on CHIKV replication. These findings collectively suggest that IFITM-2 and -3 play a pivotal role in the inhibition of CHIKV. Furthermore, based on the outcomes obtained through qRT-PCR and plaque assays, we can infer that IFITMs have an impact on both viral genome replication and the late stages of viral infection.

Expression of IFITMs modulates the human innate immune response

Next, the impact of IFITM overexpression on the innate immune system was investigated using PCR array. RNA was collected from plasmid control, IFITM1, 2, or 3 HFF-1-overexpressing cells before RT-PCR and PCR array was performed. The results were analyzed and compared with plasmid control-overexpressing HFF-1 cells (Fig. 3A). The results show that all IFITM1, 2, and 3 markedly upregulated *TLR3*, *TLR7*, *TLR8*, and *TLR9* genes and their downstream signaling molecules such as *TRADD*, *IRAK1*, *TRAF6*, and *MAP3 K7* (Fig. 3B). In the RLR signaling pathways, the overexpression of IFITMs markedly downregulated the expression of *DHX58* gene which encodes LGP2 protein, a negative regulator of retinoic acid-induced gene I (RIG-I). Conversely, it promoted the expression of *DDX58* gene which encodes RIG-I, a receptor in RLR signaling pathways. Moreover, transcription factors including interferon regulatory factor (IRF) 3/5/7, which are downstream signaling of both TLR and RLR signaling pathways^{3,4}, were upregulated in IFITMs overexpressing cells as well (Fig. 3C). For the IFNs signaling pathway, *IFNA1*, *IFNA2* and *STAT1* expression was enhanced by IFITMs, while the expression

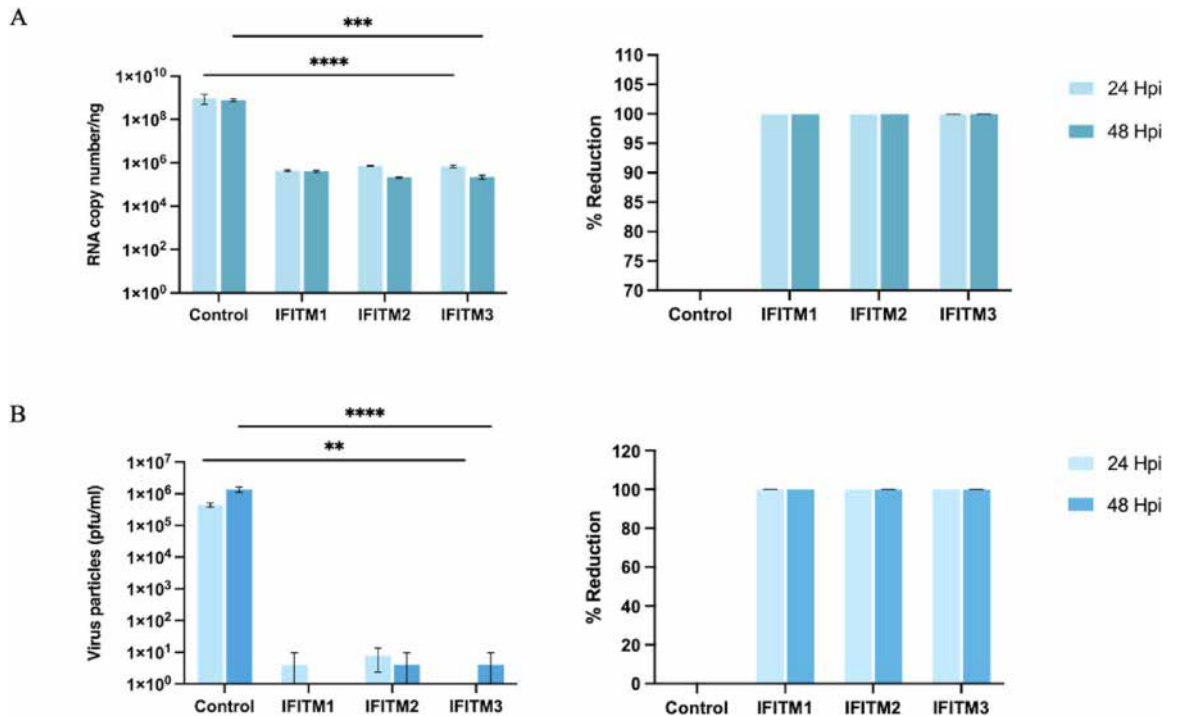


Fig. 1. IFITMs exhibit antiviral properties to CHIKV infection. HFF-1 cells were transfected with 0.1 μ g of the plasmid containing either plasmid control, IFITM1, IFITM2, or IFITM3 gene to overexpress each gene in HFF-1 cells. The cell was then infected with CHIKV at an MOI of 1 for 24 and 48 h before harvested cells lysate for quantifying (A) the viral RNA using RT-qPCR and supernatant for quantification of (B) virus particles using plaque assay. Data are presented as means \pm SD from three independent experiments. The significance of the differences among groups was evaluated by using two-way ANOVA. Statistical significance was accepted at $p < 0.05$. **= $p < 0.01$, ***= $p < 0.001$, ****= $p < 0.0001$.

of other ISGs such as *MX1* decreased (Fig. 3D). Altogether, these results imply that IFITMs modulated innate immune response mainly through at least TLR, RLR and Type I IFNs signaling pathways on human foreskin cells, as shown in Fig. 4.

Extrinsic-overexpressed IFITMs inhibit CHIKV infection via modulating innate immune responses

To examine the effects of IFITM overexpression in CHIKV-infected cells, we compared gene expression patterns of IFITM overexpressing cells infected with CHIKV with CHIKV-infected plasmid control- overexpressing cells (Fig. 5A). In contrast, CHIKV infection in upregulation of all IFITM1, 2, and 3 markedly downregulated *TLR3*, *TLR7*, *TLR8*, and *TLR9* genes as well as down-regulated other gene-encoded downstream signaling protein of TLR signaling pathways, for example, *TRADD* and *TRAF6* (Fig. 5B). On the other hand, in RLR signaling pathways, all CHIKV-infected IFITMs-overexpressing cells markedly downregulated the expression of *DHX58* gene while slightly increasing expression of *DDX58* gene. Additionally, the downstream signaling of both TLR and RLR signaling pathways, *IRF 3/5/7*, was reduced in expression after CHIKV infection (Fig. 5C). All genes involved in IFNs signaling pathway, *IFNA1*, *IFNA2*, *STAT*, *MX1* and *CXCL1*, markedly declined in their expression after cell infection (Fig. 5D). These data suggest that CHIKV attempts to impair the immune response to favor its replication mainly through TLR, RLR and Type I IFNs signaling pathways.

IFITMs extend the antiviral properties to inhibit ZIKV infection

ZIKV is another important arbovirus that circulate in several areas worldwide, like CHIKV²¹. The prior study by Monel et al., has documented that the overexpression of IFITM3 in primary human fibroblasts leads to a reduction in ZIKV infection²². However, the present investigation endeavors to validate and broaden the spectrum of antiviral properties associated with IFITM1, IFITM2, and IFITM3 against ZIKV, utilizing the HFF-1 cell lines. The HFF-1 cells transfected with either plasmid control, IFITM1, IFITM2, or IFITM3 were infected with ZIKV and quantified for viral RNA and virus particles. Interestingly, all IFITMs exert antiviral properties against ZIKV infection in human skin fibroblasts demonstrated through the reduction of viral RNA and virus particles in IFITM transfected cells compared to plasmid control- overexpressing cells. Noticeably, using RT-qPCR, IFITM2 and IFITM3 showed a stronger inhibitory effect than IFITM1 on ZIKV infection (Fig. 6A). In support of this finding, silencing of IFITM expression in HFF-1 cells enhanced ZIKV infection. Viral RNA and virus particles of ZIKV significantly increased in IFITM2 and IFITM3 knockdown cells when compared to the control (Fig. 6B). These data indicated that IFITM2 and IFITM3 extend the antiviral role to ZIKV infection.

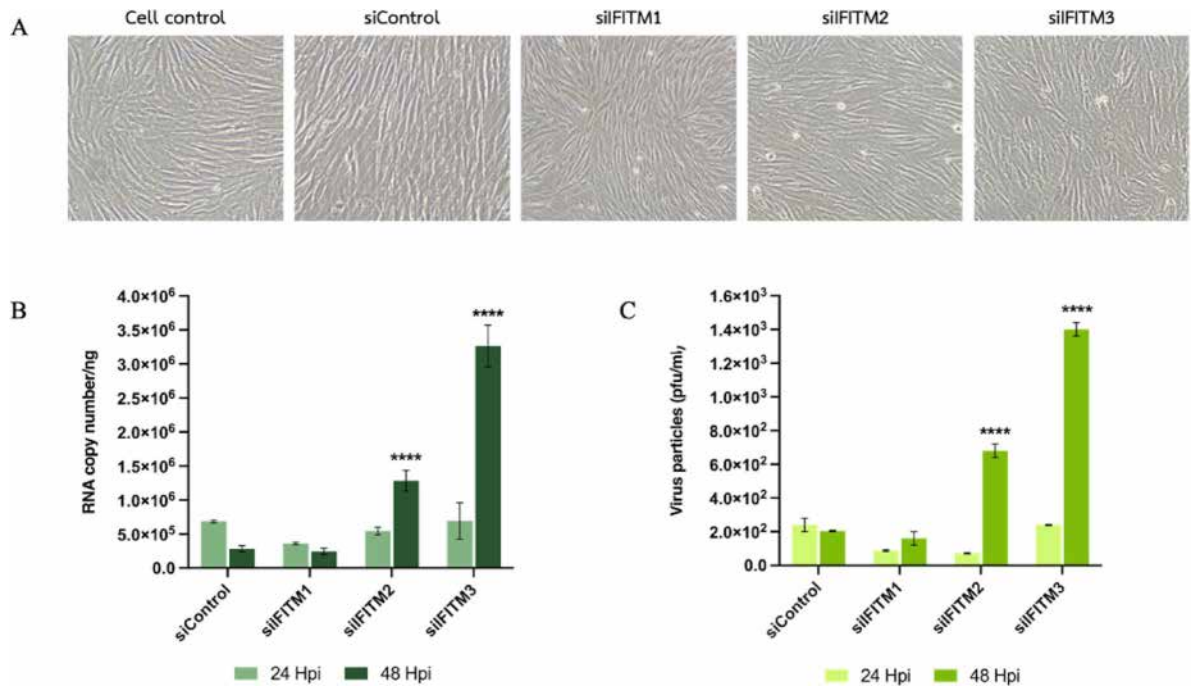


Fig. 2. Knockdown of IFITMs present antiviral properties of IFITMs against CHIKV infection. HFF-1 were transfected with 80 nM siControl and siIFITM1, siIFITM2, and siIFITM3 to knockdown the IFITMs gene. Transfected cells were (A) visually inspected to detect putative morphological changes and cell death (10x). The cells were then infected with CHIKV at a MOI of 2 for 24 and 48 h before harvested cells lysate for quantifying (B) the viral RNA using RT-qPCR and supernatant for quantification of (C) virus particles using plaque assay. Data are presented as means \pm SD from three independent experiments. The significance of the differences among groups was evaluated by using two-way ANOVA. Statistical significance was accepted at $p < 0.05$. ****= $p < 0.0001$.

Discussion

CHIKV is an arbovirus transmitted mainly by *Aedes spp.* during bite on human skin²³. Despite being a global health risk, no specific antiviral drugs and vaccines against the virus are available. However, several molecules have been studied as potential antiviral agents, including suramin²⁴, picolinic acid²⁵, imipramine²⁶ as well as ISGs, such as IFI16²⁷ and IFITMs^{28,29}. The immune-related interferon-induced transmembrane proteins, or IFITMs, have been previously reported to inhibit several viruses, including alphaviruses. Ectopic expression of IFITM2 and IFITM3 in A549 cells (human epithelial cells from lung tissue) restricted replication of alphaviruses, including Semliki Forest virus (SFV) and Sindbis virus (SINV)³⁰. Additionally, IFITM3 has been shown to play an essential role in restricting CHIKV infection both *in vitro* and *in vivo*^{28,29}.

In this study, we examined the role of IFITM1, IFITM2, and IFITM3 in CHIKV infection in human skin fibroblasts, which are among the cells initially infected in the setting of natural infection. Our results indicate that the overexpression of IFITM1, IFITM2, and IFITM3 restricts CHIKV infection in HFF-1 cells. The reduction in both viral RNA and virus particle production suggests that all IFITMs interfere with the CHIKV replication cycle. These findings are supported by the report of Lin and collaborators, which demonstrated that IFITM1 decreases host membrane fluidity with increasing interruption of the IAV-induced cell-to-cell fusion field³¹. Concomitantly, it has been reported that IFITM3 oligomers inhibit virus-cell fusion by enhancing membrane rigidity³². Changes in membrane fluidity have been shown in other studies that overexpression of IFITM proteins induced changes in the lipid packaging order of host membranes, resulting in less membrane fluidity^{31,33}. Cholesterol has also been reported to interact with IFITM proteins, altering their conformation, which is vital for the antiviral activity against IAV, SARS-CoV-2 and EBOV^{34,35}. IFITM3 has been shown to interact with vesicle-associated membrane protein-associated protein A (VAPA), disrupting cholesterol homeostasis and resulting in cholesterol accumulation in late endosomes. This accumulation inhibits endosomal fusion with the viral envelope and viral entry, restricting infections by viruses such as VSV and IAV³⁶. These observations are consistent with our previous study, demonstrating that cholesterol accumulation in the late endosome/lysosome inhibits CHIKV replication in human skin fibroblasts²⁶. These data suggest that IFITMs might inhibit CHIKV infection through the interaction with VAPA and inducing cholesterol accumulation in late endosomes, thereby inhibiting viral fusion.

Surprisingly, when HFF1 cells were deficient in IFITMs, only IFITM2 and IFITM3 could enhance the virus replication, but not IFITM1. This may be explained by the cellular localization of IFITM1 which is mainly at the plasma membrane with some distribute in cytoplasm, while IFITM2 and IFITM3 are dominantly located at the endo/lysosomal compartments (Supplementary fig. S4)³⁷, where CHIKV and ZIKV penetrate and uncoat³⁸.

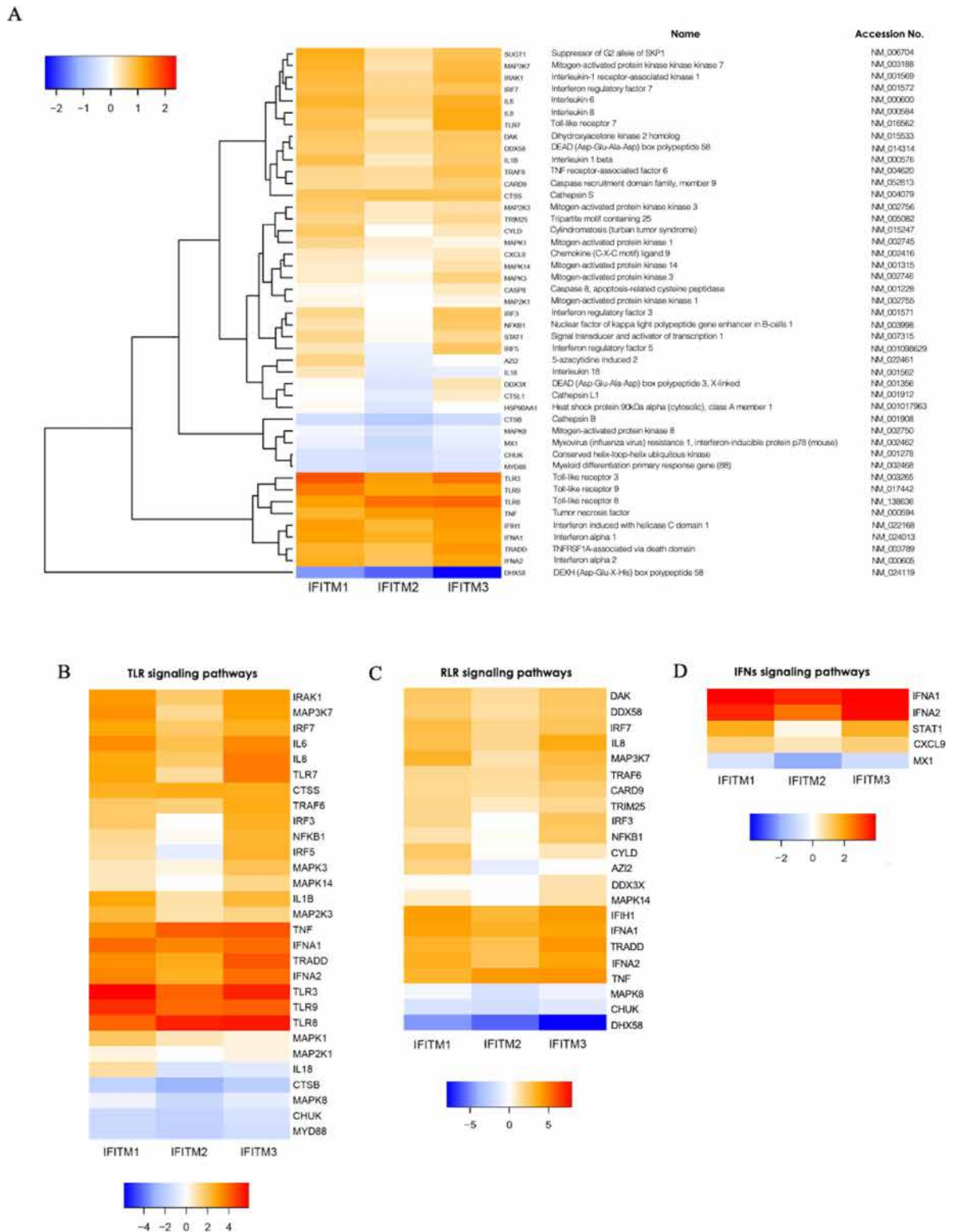


Fig. 3. Exogenous overexpression of IFITMs modulates the human innate immune response. plasmid control and IFITM1, 2, and 3 transfected were collected for RNA extraction, RT-PCR and PCR array. **(A)** The results present as fold change of gene expression compared plasmid control- overexpressing HFF-1 cells. The upregulation was shown as orange to red while the downregulation was shown as blue. Three main innate immune pathways which demonstrated to be modulated by IFITMs are separately shown as **(B)** TLR signaling pathway, **(C)** RLR signaling pathway, and **(D)** IFNs signaling pathway.

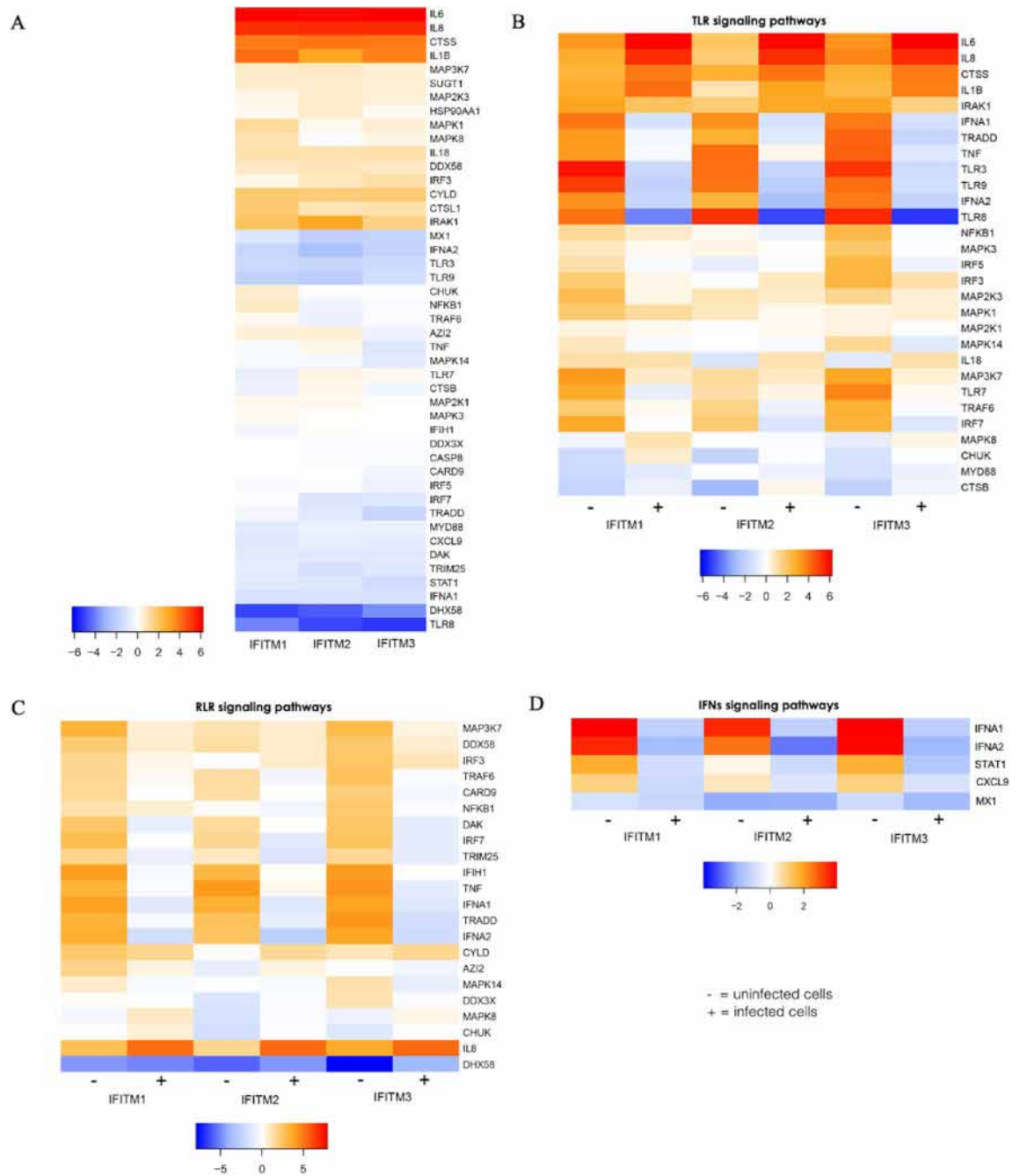


Fig. 5. CHIKV infection impairs the innate immune response in IFITMs-overexpressed HFF-1 cells. Plasmid control and IFITM1, 2, and 3 overexpressed cells were infected by CHIKV. After 48 h, the cells were collected for RNA extraction, RT-PCR and PCR array. **(A)** The results present as fold change of gene expression compared to infected-plasmid control cells. The upregulation was shown as orange to red while the downregulation was shown as blue. Three main innate immune pathways were demonstrated to be imbalanced by CHIKV including **(B)** TLR signaling pathway, **(C)** RLR signaling pathway, and **(D)** IFNs signaling pathway. - = uninfected cells, + = infected cells.

viral RNA. Activation of TLR signaling pathways leads to the expression and phosphorylation of transcription factors, including IRF3/5/7, NF- κ B, and AP-1, which further resulted in upregulated the expression of IFNs and several inflammatory cytokines^{3,4}. As demonstrated by our study, the expression of IFITMs markedly upregulates the expression of *TLR3*, *TLR7*, *TLR8* and *TLR9* in HFF1-infected cells. This upregulation of TLRs is associated with the upregulation of *IRF3/5/7*, which can potentially affect the expression of IFNs and cytokines. Moreover, the upregulation of NF- κ B, another downstream signaling protein in TLR pathway that acts as a transcription factor responsible for the expression of several inflammatory genes, has also been observed^{39,40}. These effects result in the upregulation of TNF and IL-8 in IFITMs overexpressed cells. Altogether, these data

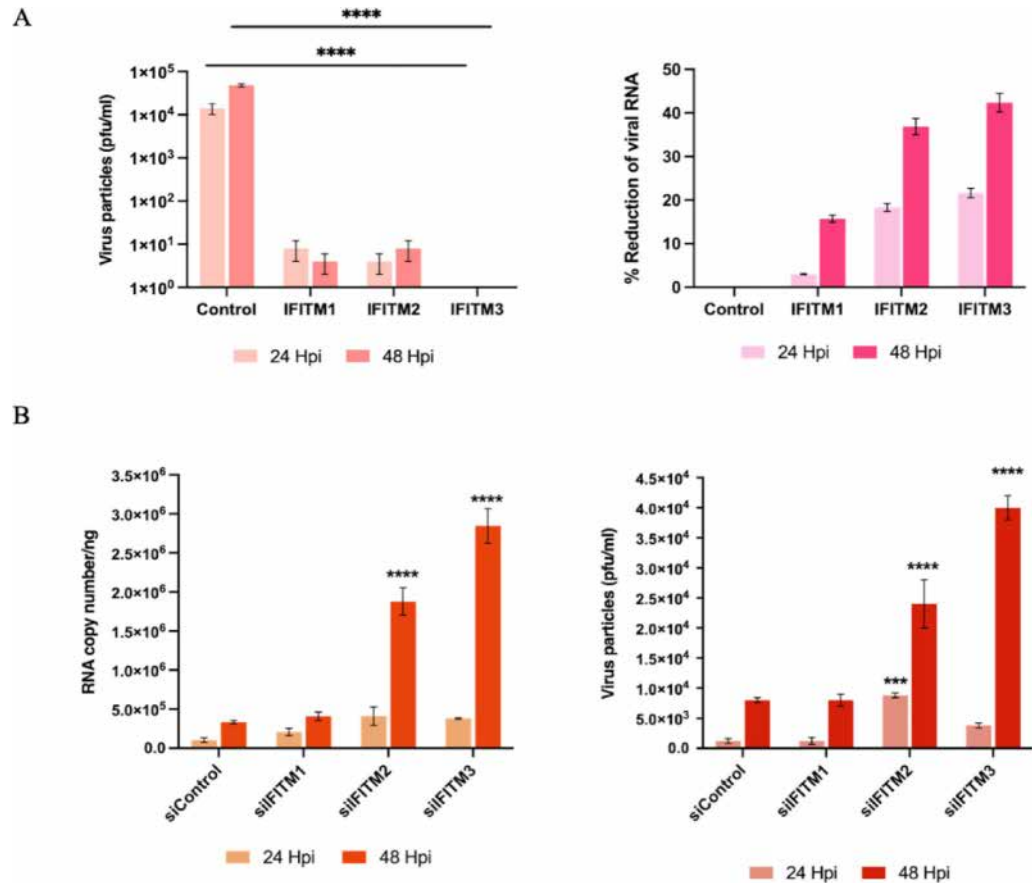


Fig. 6. IFITMs inhibit ZIKV infection on human skin cells. HFF-1 were seed and transfected with (A) plasmid containing either IFITM1, IFITM2, or IFITM3 gene and (B) siIFITM1, siIFITM2, or siIFITM3 before challenging with ZIKV at MOI of 1 and quantified the viral RNA using RT-qPCR and virus particles using plaque assay at 24 and 48 hpi. Data are presented as means \pm SD from three independent experiments. The significance of the differences among groups was evaluated by using two-way ANOVA. Statistical significance was accepted at $p < 0.05$. ***= $p < 0.001$, ****= $p < 0.0001$.

suggest that IFITMs promote the antiviral immune response to restrict CHIKV infection through activation of TLR signaling pathway. In contrast with our finding, Jiang et al. suggested that IFITM3 promotes the degradation of IRF3, limiting the type-I interferon response to Sendai virus infection⁴¹. However, it is important to note that the study used HeLa cells, which originate from the human cervix, may exhibit different responses to different types of virus infections.

The overexpression of IFITMs was also demonstrated to substantially reduce the expression of LGP2, which has been reported to act as a negative regulator of RIG-I through an unclear mechanism. It has been proposed that LGP2 interferes RIG-I signaling via competitively binding to ligands of RIG-I, binding directly to RIG-I repressor domain, or interfering with the recruitment of mitochondrial antiviral signaling (MAVS), a downstream signaling protein of RIG-I, by forming a protein interaction⁴². Therefore, downregulation of LGP2 expression could suggest increasing antiviral response through RIG-I and RIG-I-like receptor (RLR) signaling pathways. In the RLR signaling pathway, not only does LGP2 respond to IFITMs expression, but RIG-I is also shown to be upregulated. RIG-I is one of the receptors in RLR signaling pathway that can recognize viral RNA and trigger downstream signaling to respond to viral infection, resulting in the expression of transcription factors involving IRF3/7 and NF- κ B, and ultimately stimulating IFNs and cytokines production^{3,4}.

For the IFNs signaling pathway, in this finding, interferon alpha-1 and -2 (IFNA1 and IFNA2) are upregulated in all IFITM overexpressing cells, which might be due to the increasing antiviral response through TLR and RLR signaling pathway. Our discovery is substantiated by a recent study conducted by Chen and colleagues, demonstrating that IFITM2 elicits an antiviral response through augmentation of the type I interferon (IFN) signaling pathway⁴³. The secreted IFNs from infected cells can result in the phosphorylation of tyrosine kinase 2, JAK1 and STAT1 and 2 proteins. The activated STAT1 and STAT2 further interact with interferon regulatory factor 9 (IRF-9) to form IFN-stimulated genes factor 3 (ISGF-3) complex, which then binds to interferon-stimulated response elements (ISREs) on the promoter of IFN-stimulated genes (ISGs), resulting in expression of ISGs that exhibit antiviral activity through various mechanisms⁵. The increase in gene expression of IFNA1, IFNA2, and STAT1 reported in this study could suggest the promotion of IFN signaling, which finally resulted in the upregulation of many ISGs, such as CXCL9, aiding in restricting viral infection. While Shi and colleagues

found that IFNA is suppressed when IFITM2 is overexpressed, and the gene is enhanced when IFITM2 is knocked out in Huh7 cells⁴⁴. These discrepancies may have occurred because the study utilized a different model of cell line and virus. However, some ISGs, including MX1, were demonstrated to be downregulated in IFITMs overexpressed cells via unknown mechanism. Since we investigated the effect of IFITMs on only a few ISGs and studies on the impact of IFITMs on other ISGs remain limited, further studies on this aspect are still required to better understand and confirm IFITMs' effect on promoting the IFNs signaling pathway.

Considering the modulation of gene expression in the innate immune response by IFITMs, it was shown that some genes have effects at different types and levels of alteration between each IFITM, indicating various activities and properties among these immune-related IFITM proteins. These may raise a reason that CHIKV was inhibited at a different level in each IFITM-overexpressed cell. However, the mechanism underlying the alteration is one of the interesting points that should be further investigated.

Conclusion

In conclusion, this study reports the antiviral activity of IFITMs against CHIKV in human skin fibroblast. Based on our findings, we propose several antiviral mechanisms of IFITMs on CHIKV infection in human fibroblasts (Fig. 7). IFITMs might inhibit the virus replication through the inducing accumulation of cholesterol to block viral fusion and act as a host-targeting antiviral agent to modulate the expression of genes involved in antiviral innate immune response, especially TLRs and LGP2 which could help in the promotion of TLR and RLR signaling resulting in IFNs production. Moreover, IFITMs expression also promotes STAT1 expression which could activate type I IFN signaling pathway, leading to increased transcription of ISGs in human skin fibroblast. We also demonstrated the inhibitory effect of IFITMs on another arbovirus, ZIKV, in these cells. However, the exact mechanism of IFITM-induced viral fusion blocking needs to be investigated. Our study provides an additional aspect of IFITMs' properties to act as antiviral agent against arbovirus infection.

Materials and methods

Cells and viruses

The Vero cells line (African green monkey kidney cells; ATCC[®] CCL-81™) and HFF-1 cells line (Human skin fibroblast cells; ATCC[®] SCRC-1041™) were cultured in High Glucose Dulbecco's modified Eagle's Minimum Essential Medium (DMEM; Cytiva, Logan, Utah) supplemented with 10% and 15% heat-inactivated fetal bovine serum (FBS; Gibco, Paisley, UK), respectively. The C6/36 (Aedes Albopictus cells; ATCC[®] CRL-1660™) grown in L-15 Medium (Leibovitz) supplemented with 10% tryptose phosphate broth (TPB, Sigma-Aldrich, MO, USA) and 10% FBS. Vero and HFF-1 cells were maintained in a humidified 37 °C incubator with 5% CO₂ while

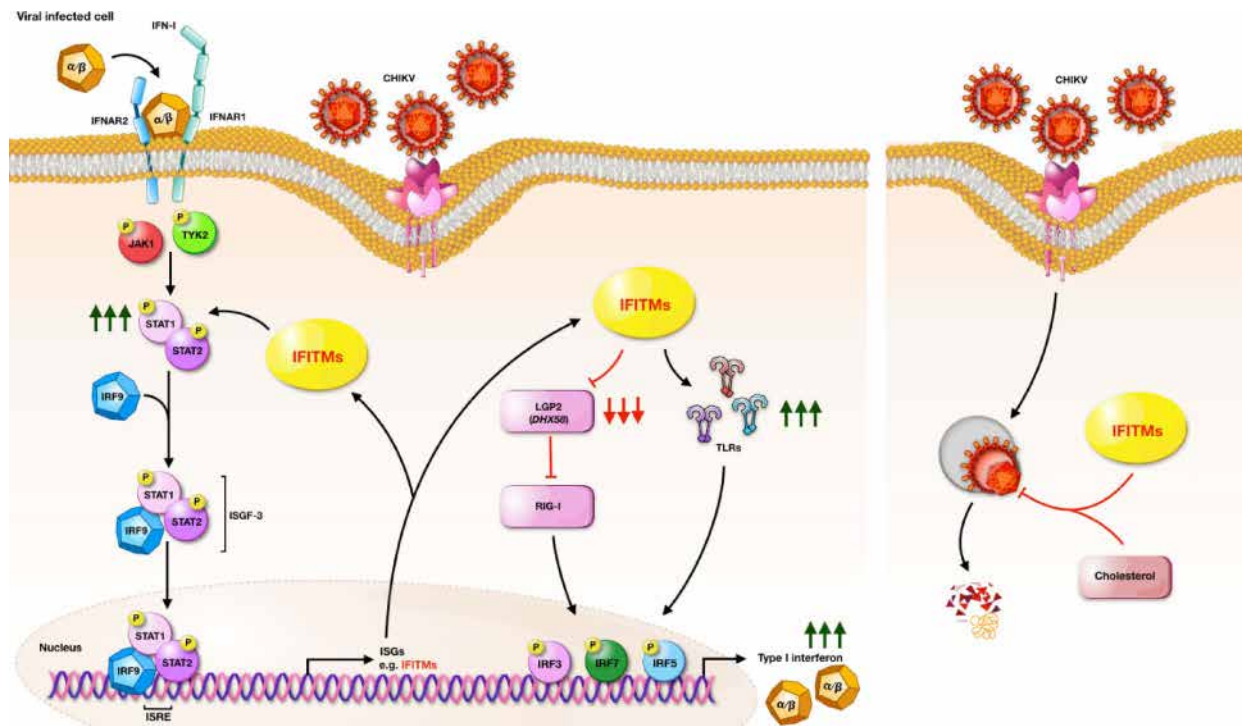


Fig. 7. Proposed mechanism of IFITMs on CHIKV infection in human dermal cells. IFITMs expression in response of viral infection downregulated the expression of LGP2 and upregulated the expression of TLRs resulting in increasing type I interferon expression. IFITMs also upregulated the expression of STAT1 in IFNs signaling pathway which could further induced ISGs expression that can act against viral infection. Moreover, IFITMs in corresponding with cholesterol could inhibit the fusion step of viral replication restricted the viral infection. Figure was created using Keynote version 9.1 (<https://www.apple.com/keynote/>).

C6/36 were maintained in 28 °C incubator. CHIKV, LR2006_OPY1 strain (isolated from a viremic patient in La Réunion Island in 2006), was received from Dr. Philippe Desprès (PIMIT, Inserm U1187, St Clotilde) while the clinical isolate PF-25013-18of ZIKV has been previously described²⁰. The CHIKV and ZIKV were grown in C6/36 cells at 28 °C and kept at –80 °C until used.

Plasmids and reagents

Plasmids encoding IFITM1, IFITM2 and IFITM3 proteins were kind gifts from Pr P. Kellam (Wellcome Trust Sanger Institute, Wellcome Trust Genome Campus, UK). Small interfering RNA (siRNA) of IFITM1, 2, and 3 (siIFITM1, 2, and 3) and non-silencing control siRNA (siControl) were purchased from QIAGEN (Maryland, USA). The target sequence of siControl, IFITM1 IFITM2, and IFITM3 are shown in Table 1.

Overexpression and small interfering RNA (siRNA) transfection

After seeding of HFF-1 cells in six-well plates for 24 h, plasmids containing IFITM1, IFITM2, or IFITM3 were transfected with Lipofectamine™ 3000 (Invitrogen, CA, USA) according to the manufacturer's protocol to overexpress each gene in HFF-1 cells while small interfering RNA (siRNA) of IFITM1, 2, and 3 (siIFITM1, 2, and 3) at a concentration of 80 nM in the final volume of transfection were transfected with Lipofectamine™ RNAiMAX (Invitrogen, CA, USA) following the manufacturer's protocol to knockdown each IFITMs. Then, the transgene expressions were evaluated by Western blot analysis and RT-qPCR.

Viability assay

The MTT-based assay was used to determine cell viability. Briefly, cells were transfected with IFITMs plasmids using Lipofectamine™ 3000 according to the manufacturer's protocol and incubated at 37 °C, 5% CO₂ for 24 h. Then, cells were washed with phosphate-buffered saline (PBS; Gibco, Paislay, UK) and incubated with 100 µL MTT. After 2 h, MTT was removed, 50 µL of DMSO was added and incubated at 37 °C for 10 min. Finally, the absorbances were measured at 570 nm in order to determine cell viability.

Gene expression by quantitative reverse transcription polymerase chain reaction (RT-qPCR)

Total RNA was extracted from human fibroblasts. The reactions were carried out using 0.25 µg of total RNA as a template. The reaction was carried out using 1 µg total RNA as template for the normalization of viral RNA to the amount of total RNA. The Maxima™ Probe/ROX qPCR Master Mix (2×) (Thermo Scientific) was used in qPCR experiment. Each reaction of 25 µL contained 400 nM of each primer, 200 nM of specific probe and 1× Maxima™ Probe/ROX qPCR Master Mix. Primers sequences are listed in Table 2. The amplification conditions were 95 °C for 10 min followed by 45 amplification cycles of 95 °C for 15 s, 60 °C for 20 s and 72 °C for 30 s. The reactions were performed in an Applied Biosystem 7300 system. Real time data were analyzed using the SDS software (Thermo Fischer Scientific). GAPDH was used as endogenous control for calculation of relative fold change.

Western blot analysis

Total proteins were collected from human fibroblasts using a RIPA buffer supplemented with a protease inhibitor cocktail solution (Calbiochem, MA, USA). Protein concentrations were determined by using a NanoDrop Spectrophotometer. Equal amounts of proteins were separated by sodium dodecyl sulfate-polyacrylamide gel electrophoresis (SDS-PAGE) and then transferred to a PVDF (polyvinylidene difluoride) membrane for immunoblotting. Membranes were blocked with 5% non-fat dry milk in phosphate-buffered saline with 0.05% Tween 20 (PBST) for 2 h and incubated overnight with primary antibodies followed by washing with PBST and incubated in the dark with horseradish peroxidase (HRP)-conjugated secondary antibodies (Cell Signaling Technology, Inc) at room temperature for 1 h. The proteins were then visualized using a SuperSignal™ West Pico chemiluminescent substrate kit (Thermo Scientific, IL, USA). Finally, the membrane was stripped and re-probed with an anti-β-actin antibody to ensure that equivalent protein levels were loaded in each lane.

Product name	Target sequence
siControl	AATTCTCCGAACGTGTCACGT
Hs_IFITM1_1	CCTGTCTACAGTGTCATTCAA
Hs_IFITM1_2	ACCATATTATGTTACAGATAA
Hs_IFITM1_5	ACAGTCTACCATATTATGTTA
Hs_IFITM1_9	TCCAAGGTCCACCGTGATCAA
Hs_IFITM2_1	ACCATGAACCACATTGTGCAA
Hs_IFITM2_4	CAGCGATAGATCAGGAGGCAT
Hs_IFITM2_5	TCCCACGTACTCTATCTCCA
Hs_IFITM2_8	CTGGTGCTGCTGTGACTTCAA
Hs_IFITM3_5	TCCCACGTACTCCAACTTCCA
Hs_IFITM3_6	AGGAAACTGTTGAGAAACCGA
Hs_IFITM3_7	GCACGTGTTTCTGGTGCTAAA
Hs_IFITM3_8	TCCAGGCCTATGGATAGATCA

Table 1. Target sequence of SiControl, IFITM1, IFITM2 and IFITM3.

Genes	Primers	Sequence (5'->3')
IFITM1	IFITM1-F	5'ACTCCGTGAAGTCTAGGGACA3'
	IFITM1-R	5'TGTCCAGAGCCGAATACCAG3'
IFITM2	IFITM2-F	5'ATCCCGGTAACCCGATCAC3'
	IFITM2-R	5'CTTCTGTCCCTAGACTTCAC3'
IFITM3	IFITM3-F	5'GGTCTTCGCTGGACACCAT3'
	IFITM3-R	5'TGTCCCTAGACTTCACGGAGTA3'

Table 2. Primers of IFITM1, IFITM2 and IFITM3.

Virus	Primer	Sequence (5'->3')
CHIKV	CHIKV-F	5'AAGCT(CT)CGCGTCCTTACCAAG3'
	CHIKV-R	5'CCAAATTGTCC(CT)GGTCTTCCT3'
ZIKV	ZIKV-F	5'TTGGTCATGATACTGCTGATTGC3'
	ZIKV-R	5'CCTTCCACAAAGTCCCTATTGC3'

Table 3. Primers for viral detection used in this study.

Viral infection

Cells were washed with PBS and the cells were incubated with CHIKV or ZIKV at the desired multiple of infection (MOI) for 2 h at 37 °C with 5% CO₂ while gently agitating the plates. Then, the inoculum was removed, the cells were washed with PBS and DMEM supplemented with 15% FBS was added. Plates were incubated at 37 °C with 5% CO₂ for 24 and 48 h before collecting supernatants and cell lysis for virus particle and viral genome quantification, respectively.

Plaque assay

Confluent Vero cells monolayer were prepared in 24-well tissue culture plates at 2.5×10^5 cells/well for 24 h. Viruses were diluted by making a serial 10-fold dilution with 1X DMEM. Each virus concentration was transferred to monolayer cells and incubated at 37 °C with 5% CO₂ for 90 min for ZIKV and 2 h for CHIKV, continuously mixing for viral adsorption. The inoculums were discarded then infected cells were washed with 1X PBS and overlaid with 2.4% carboxyl methyl cellulose, subsequently incubated at 37 °C with 5% CO₂ for 7 days for ZIKV and 3 days for CHIKV. Plaques were counted after fixing with 3.7% formaldehyde for 30 min and staining with 0.5% Crystal violet in 20% ethanol for 1 h. The virus titer will be calculated and presented as a plaque-forming unit per milliliter (PFU/mL).

-qPCR

2 µL of total RNA extracted from human fibroblasts were used as a template for RT-qPCR using the KAPA SYBR FAST One-Step (KAPA Biosystem, Cape town, South Africa). Each reaction of 10 µL contained 2 µM of each primer (Table 3), 5 µL of KAPA SYBR FAST qPCR, and 0.2 µL of RT Mix. The amplification conditions were 42 °C for 10 min and 95 °C for 3 min followed by 45 amplification cycles of 95 °C for 10 s, 58 °C for 20 s, and 72 °C for 30 s. Reactions were performed in a CFX96 Real-Time System, C1000 Touch Thermal cycler (Bio-Rad). Viral RNA was quantified by comparing each virus's threshold cycle (Ct) values with the RNA standard curve.

RT²

Total RNA extracted from human fibroblasts was reverse transcript to cDNA using the iScript™ Reverse Transcription Supermix for RT-qPCR (Bio-Rad, USA) according to the manufacturer's instructions. Then cDNA was analyzed by RT²Profiler PCR Arrays Antiviral response (PAHS-122Z; QIAGEN, Maryland, USA). The 8 µL of cDNA was mixed with 650 µL of 2x RT SYBR Green Mastermix and 642 µL of RNase-free water before adding into the 384-well RT² Profiler PCR Array plate under the supporting of 384EZLoad Cover for profiling expression of total 84 genes of human antiviral response, as described in the manufacturer's handbook. The DNA amplification was carried out with the Roche LightCycler 480 real time cycler using a cycling program of 95 °C for 10 min, followed by 45 cycles of 95 °C for 15 s and 60 °C for 1 min before a melting curve acquisition step. The fold changes of gene expression in each condition were calculated in comparison to the values of controls.

Data analysis and statistical methods

Data are presented as means ± SD. The significance of the differences among groups was evaluated using the two-way ANOVA. Statistical significance was accepted at $p < 0.05$.

Data availability

The data that support the findings of the study are available within the article. Additional data are available upon request from the corresponding author.

Received: 23 March 2024; Accepted: 29 April 2025

Published online: 06 May 2025

References

1. Thiberville, S. D. et al. Chikungunya fever: epidemiology, clinical syndrome, pathogenesis and therapy. *Antiviral Res.* **99**, 345–370 (2013).
2. Wichit, S. et al. Chikungunya and Zika viruses: Co-Circulation and the interplay between viral proteins and host factors. *Pathogens* **10**, 448 (2021).
3. Kusiak, A. & Brady, G. Bifurcation of signalling in human innate immune pathways to NF- κ B and IRF family activation. *Biochem. Pharmacol.* **205**, 115246 (2022).
4. Singh, H., Koury, J. & Kaul, M. Innate immune sensing of viruses and its consequences for the central nervous system. *Viruses* **13**, 170 (2021).
5. Platanias, L. C. Mechanisms of type-I- and type-II-interferon-mediated signalling. *Nat. Rev. Immunol.* **5**, 375–386 (2005).
6. Infusini, G. et al. Respiratory DC use IFITM3 to avoid direct viral infection and safeguard Virus-Specific CD8+ T cell priming. *PLoS ONE*. **10**, e0143539 (2015).
7. Hachim, M. Y. et al. Interferon-Induced transmembrane protein (IFITM3) is upregulated explicitly in SARS-CoV-2 infected lung epithelial cells. *Front. Immunol.* **11**, (2020).
8. Zhou, Z. et al. Heightened innate immune responses in the respiratory tract of COVID-19 patients. *Cell. Host Microbe*. **27**, 883–890e2 (2020).
9. Friedman, R. L., Manly, S. P., McMahon, M., Kerr, I. M. & Stark, G. R. Transcriptional and posttranscriptional regulation of interferon-induced gene expression in human cells. *Cell* **38**, 745–755 (1984).
10. Reid, L. E. et al. A single DNA response element can confer inducibility by both alpha- and gamma-interferons. *Proc. Natl. Acad. Sci. U S A*. **86**, 840–844 (1989).
11. Alber, D. & Staeheli, P. Partial Inhibition of vesicular stomatitis virus by the interferon-induced human 9–27 protein. *J. Interferon Cytokine Res.* **16**, 375–380 (1996).
12. Lin, T. Y. et al. Amphotericin B increases influenza A virus infection by preventing IFITM3-Mediated restriction. *Cell. Rep.* **5**, 895–908 (2013).
13. Muñoz-Moreno, R. et al. Antiviral role of IFITM proteins in African swine fever virus infection. *PLoS One*. **11**, e0154366 (2016).
14. Compton, A. A. et al. IFITM proteins incorporated into HIV-1 virions impair viral fusion and spread. *Cell. Host Microbe*. **16**, 736–747 (2014).
15. Huang, I. C. et al. Distinct patterns of IFITM-mediated restriction of filoviruses, SARS coronavirus, and influenza A virus. *PLoS Pathog.* **7**, e1001258 (2011).
16. Wrensch, F., Winkler, M. & Pöhlmann, S. IFITM proteins inhibit entry driven by the MERS-coronavirus Spike protein: evidence for cholesterol-independent mechanisms. *Viruses* **6**, 3683–3698 (2014).
17. Stacey, M. A. et al. The antiviral restriction factor IFN-induced transmembrane protein 3 prevents cytokine-driven CMV pathogenesis. *J. Clin. Invest.* **127**, 1463–1474.
18. Yáñez, D. C. et al. IFITM proteins drive type 2 T helper cell differentiation and exacerbate allergic airway inflammation. *Eur. J. Immunol.* **49**, 66–78 (2019).
19. Couderc, T. et al. A mouse model for Chikungunya: young age and inefficient Type-I interferon signaling are risk factors for severe disease. *PLoS Pathog.* **4**, e29 (2008).
20. Hamel, R. et al. Biology of Zika virus infection in human skin cells. *J. Virol.* **89**, 8880–8896 (2015).
21. Raksakoon, C. & Potiwat, R. Current arboviral threats and their potential vectors in Thailand. *Pathogens* **10**, 80 (2021).
22. Monel, B. et al. Zika virus induces massive cytoplasmic vacuolization and paraptosis-like death in infected cells. *EMBO J.* **36**, 1653–1668 (2017).
23. Wichit, S. et al. Aedes Aegypti saliva enhances Chikungunya virus replication in human skin fibroblasts via Inhibition of the type I interferon signaling pathway. *Infect. Genet. Evol.* **55**, 68–70 (2017).
24. Ho, Y. J. et al. Suramin inhibits Chikungunya virus entry and transmission. *PLoS One*. **10**, e0133511 (2015).
25. Sharma, R. et al. Inhibition of Chikungunya virus by picolinate that targets viral capsid protein. *Virology* **498**, 265–276 (2016).
26. Wichit, S. et al. Imipramine inhibits Chikungunya virus replication in human skin fibroblasts through interference with intracellular cholesterol trafficking. *Sci. Rep.* **7**, 3145 (2017).
27. Wichit, S. et al. Interferon-inducible protein (IFI) 16 regulates Chikungunya and Zika virus infection in human skin fibroblasts. *EXCLI J.* **18**, 467–476 (2019).
28. Franz, S. et al. Human IFITM3 restricts Chikungunya virus and Mayaro virus infection and is susceptible to virus-mediated counteraction. *Life Sci. Alliance*. **4**, e20200909 (2021).
29. Poddar, S., Hyde, J. L., Gorman, M. J., Farzan, M. & Diamond, M. S. The Interferon-Stimulated gene IFITM3 restricts infection and pathogenesis of arthritogenic and encephalitic alphaviruses. *J. Virol.* **90**, 8780–8794 (2016).
30. Weston, S. et al. Alphavirus restriction by IFITM proteins. *Traffic* **17**, 997–1013 (2016).
31. Guo, X. et al. Interferon-Induced transmembrane protein 3 blocks fusion of diverse enveloped viruses by altering mechanical properties of cell membranes. *ACS Nano*. **15**, 8155–8170 (2021).
32. Rahman, K. et al. Homology-guided identification of a conserved motif linking the antiviral functions of IFITM3 to its oligomeric state. *Elife* **9**, e58537 (2020).
33. Li, K. et al. IFITM proteins restrict viral membrane hemifusion. *PLoS Pathog.* **9**, e1003124 (2013).
34. Das, T. et al. S-Palmitoylation and sterol interactions mediate antiviral specificity of IFITMs. *ACS Chem. Biol.* **17**, 2109–2120 (2022).
35. Rahman, K. et al. Cholesterol binds the amphipathic Helix of IFITM3 and regulates antiviral activity. *J. Mol. Biol.* **434**, 167759 (2022).
36. Amini-Bavil-Olyaei, S. et al. The antiviral effector IFITM3 disrupts intracellular cholesterol homeostasis to block viral entry. *Cell. Host Microbe*. **13**, 452–464 (2013).
37. Narayana, S. K. et al. The Interferon-induced transmembrane proteins, IFITM1, IFITM2, and IFITM3 inhibit hepatitis C virus entry. *J. Biol. Chem.* **290**, 25946–25959 (2015).
38. Hoornweg, T. E. et al. Dynamics of Chikungunya virus cell entry unraveled by Single-Virus tracking in living cells. *J. Virol.* **90**, 4745–4756 (2016).
39. Lawrence, T. The nuclear factor NF- κ B pathway in inflammation. *Cold Spring Harb Perspect. Biol.* **1**, a001651 (2009).
40. Pei, L. et al. Lapiferin protects against H1N1 virus-induced pulmonary inflammation by negatively regulating NF- κ B signaling. *Braz J. Med. Biol. Res.* **53**, e9183 (2020).
41. Jiang, L. Q. et al. IFITM3 inhibits virus-triggered induction of type I interferon by mediating autophagosome-dependent degradation of IRF3. *Cell. Mol. Immunol.* **15**, 858–867 (2018).
42. Quicke, K. M., Diamond, M. S. & Suthar, M. S. Negative regulators of the RIG-I-like receptor signaling pathway. *Eur. J. Immunol.* **47**, 615–628 (2017).
43. Chen, L. et al. IFITM2 presents antiviral response through enhancing type I IFN signaling pathway. *Viruses* **15**, 866 (2023).

44. Shi, Y. et al. Exosomal interferon-Induced transmembrane protein 2 transmitted to dendritic cells inhibits interferon alpha pathway activation and blocks Anti-Hepatitis B virus efficacy of exogenous interferon alpha. *Hepatology* **69**, 2396–2413 (2019).

Acknowledgment

We would like to thank Dr. Thanyakorn Rongsawat for his technical assistance.

Author contributions

Conceptualization: N.G., P.K., C.P., A.S., D.M. and S.W; Experiments: N.G., A.D., P.M.S.V, W.K., T.S., S.Y., R.H. and S.W; Writing-original draft preparation: N.G., P.M.S.V, P.S. and S.W; review and editing: N.G., P.M.S.V, T.S., S.Y., R.H., P.K., C.P., A.S., D.M., P.S. and S.W; supervision, S.W. All authors have read and agreed to the published version of the manuscript. Authorship is limited to those who have contributed substantially to work reported. We would like to thank Dr. Thanyakorn Rongsawat for his technical assistance.

Funding

This work was financially supported by the National Research Council of Thailand (NRCT): NRCT5-RGJ63012-125, Grant No. RGNS 64–172 by Office of the Permanent Secretary, Ministry of Higher Education, Science, Research and Innovation, Science, Research and Innovation (MHESI), Walailak University (Contract No. Wu-CGS-62002). This research project is supported by Mahidol University (MU's Strategic Research Fund): Fiscal year 2023, MU-SRF-RS-05 A/66. This work was also funded by the French National Research Agency #ANR-17-CE15-00029 and ANR-12-BSV3-0004”.

Declarations

Competing interests

The authors declare no competing interests.

Additional information

Supplementary Information The online version contains supplementary material available at <https://doi.org/10.1038/s41598-025-00663-6>.

Correspondence and requests for materials should be addressed to S.W.

Reprints and permissions information is available at www.nature.com/reprints.

Publisher's note Springer Nature remains neutral with regard to jurisdictional claims in published maps and institutional affiliations.

Open Access This article is licensed under a Creative Commons Attribution-NonCommercial-NoDerivatives 4.0 International License, which permits any non-commercial use, sharing, distribution and reproduction in any medium or format, as long as you give appropriate credit to the original author(s) and the source, provide a link to the Creative Commons licence, and indicate if you modified the licensed material. You do not have permission under this licence to share adapted material derived from this article or parts of it. The images or other third party material in this article are included in the article's Creative Commons licence, unless indicated otherwise in a credit line to the material. If material is not included in the article's Creative Commons licence and your intended use is not permitted by statutory regulation or exceeds the permitted use, you will need to obtain permission directly from the copyright holder. To view a copy of this licence, visit <http://creativecommons.org/licenses/by-nc-nd/4.0/>.

© The Author(s) 2025